Langmuir

Article

pubs.acs.org/Langmuir

Hollow Colloidosomes Prepared Using Accelerated Solvent Evaporation

Nur Nabilah Shahidan,[†,‡] Ruixue Liu,[†,§] Sineenat Thaiboonrod,[†] Cameron Alexander,[∥] Kevin M. Shakesheff,[∥] and Brian R. Saunders*[,†]

[†]Biomaterials Research Group, School of Materials, The University of Manchester, Grosvenor Street, Manchester, M13 9PL, United Kingdom

[‡]Faculty of Earth Science, Universiti Malaysia Kelantan, Kota Bharu, Malaysia

[§]Zhengzhou University of Light Industry, Zhengzhou, 450002, P.R. China

[∥]School of Pharmacy, The University of Nottingham, University Park, Nottingham, NG7 2 RD, United Kingdom

Supporting Information

ABSTRACT: We demonstrate a new, scalable, simple, and generally applicable two-step method to prepare hollow colloidosomes. First, a high volume fraction oil-in-water emulsion was prepared. The oil phase consisted of CH_2Cl_2 containing a hydrophobic structural polymer, such as polycaprolactone (PCL) or polystyrene (PS), which was fed into the water phase. The water phase contained poly(vinylalcohol), poly(*N*-isopropylacrylamide), or a range of cationic graft copolymer surfactants. The emulsion was rotary evaporated to rapidly remove CH_2Cl_2. This caused precipitation of PCL or PS particles which became kinetically trapped at the periphery of the droplets and formed the shell of the hollow colloidosomes. Interestingly, the PCL colloidosomes were birefringent. The colloidosome yield increased and the polydispersity decreased when the preparation scale was increased. One example colloidosome system consisted of hollow PCL colloidosomes stabilized by PVA. This system should have potential biomaterial applications due to the known biocompatibility of PCL and PVA.

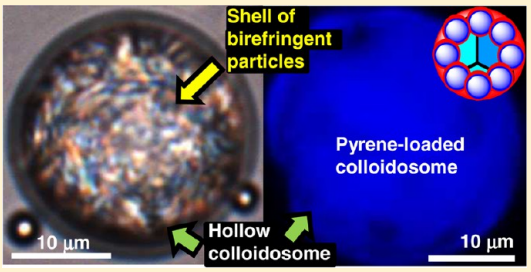

INTRODUCTION

Colloidosomes are an important subgroup of microcapsules whose shells consist of coagulated or fused colloid particles.[1] They were first reported by Velev et al.[2] Microcapsules and colloidosomes have attracted considerable interest[3−12] and have potential applications in fragrance and color release, low density thermal insulation,[13,14] opacifying agents, as well as drug delivery.[1] Microcapsule preparation usually involves a number of steps[15] that can be time-consuming. Loxley and Vincent used thermodynamic incompatibility between the polymer and a low volatility cosolvent to drive microcapsule formation.[4] Microcapsules have also been prepared by a water-in-oil (W/O) emulsion route.[14] Kim et al. prepared microcapsules using an oil-in-water (O/W) emulsion route.[16] Microcapsules have also been prepared using electrospraying.[17] Because colloidosomes contain fused colloid particles in the shells they offer additional potential for release compared to conventional microcapsules. Although a simple, scalable, and general method for colloidosome preparation method would be highly desirable, this is currently lacking from the literature to our knowledge. Here, we introduce such a method and investigate the hypothesis that hollow colloidosomes can be prepared by kinetic trapping of precipitated polymer particles within oil droplets of an O/W emulsion.

Stimulus responsive colloidosomes and microcapsules have also attracted considerable interest. pH-responsive cross-linked microcapsules have been reported by several groups.[15,18] Horecha et al.[14] used a water-in-oil preparation route to prepare thermally responsive poly(*N*-isopropylacrylamide) (PNP) microcapsules. Colloidosomes based on poly(caprolactone) (PCL) have potential application in delivery or regenerative medicine because the polymer is biodegradable. They have been previously prepared using PCL-based copolymers.[19,20] Those routes require time-consuming copolymer synthesis. Here, colloidosomes were prepared containing shells of partially fused PCL particles (Scheme 1). They were prepared using a conventional polymer surfactant (poly(vinylalcohol), PVA) and four thermally responsive polymer surfactants as well as PNP.

Our method to prepare colloidosomes started with the preparation of a concentrated O/W emulsion using a feed of CH_2Cl_2/structural polymer solution. We used oil phase volume fractions (ϕ_o) of up to 0.67 which promoted partial aggregation and adsorption of small droplets at the surface of larger droplets, coalescence, and colloidosome formation. Rotary

Received: April 23, 2013
Revised: September 26, 2013
Published: October 10, 2013

Scheme 1. Preparation of Colloidosomes Using Accelerated Solvent Evaporation[a]

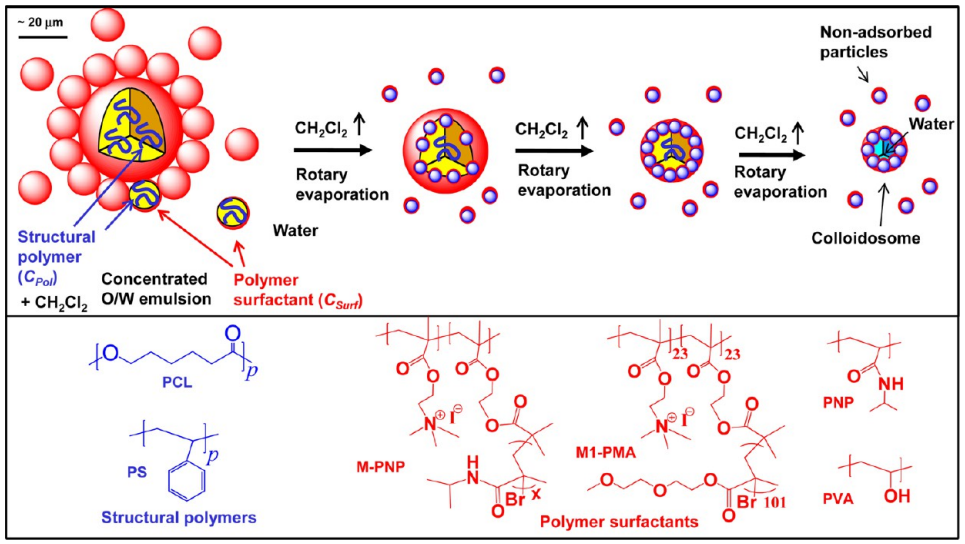

[a]The parameters C_{Pol} and C_{Surf} represent the structural polymer and polymer surfactant concentration, respectively.

evaporation was used to accelerate solvent evaporation. As the CH_2Cl_2 evaporated from the larger droplets, polymer precipitation occurred at their peripheries. Accelerated CH_2Cl_2 evaporation coupled with an increased local viscosity prevented equilibration of the polymer concentration throughout the large droplets. Due to CH_2Cl_2 removal, the polymer-deficient cores of the droplets filled with water. In contrast to other approaches, our method did not require preformed stabilizing particles[10,11] or addition of binding species.[2] It is a rapid, convenient, and scalable approach that uses standard laboratory equipment. Importantly, an example PCL/PVA colloidosome system was prepared using commercially available materials. This is a good candidate for future biomaterial applications. We also extended our method to polystyrene (PS) to further demonstrate its generality. An unexpected result from this study was that the colloidosomes were birefringent, and this is discussed.

EXPERIMENTAL SECTION

Reagents. CH_2Cl_2 (98%), pyrene (99%), and PS with a weight-average molecular weight (M_w) of 35 kg/mol were purchased from Aldrich and used as received. Polycaprolactone diol (PCL−OH) with a number-average molecular weight (M_n) of 2 kg/mol and PCL with M_n values of 10 kg/mol (PCL10, M_w/M_n = 1.4) and 80 kg/mol (PCL80, M_n = 70−90 kg/mol) were purchased from Aldrich and used as received. PVA (98% hydrolyzed, M_n = 13−28 kg/mol) and PNP (M_w = 19−30 kg/mol) were purchased from Aldrich and used as received. Water was Milli-Q grade quality.

Polymer Surfactants. For most of this study two families of cationic thermally responsive graft copolymer surfactants were used (M-PNP and M1-PMA) (see Scheme 1). They were prepared using atom transfer radical polymerization (ATRP) and macroinitiators (M1 and M2) containing quaternarized *N,N*-dimethylaminoethyl methacrylate units (DMA^+).[21,22] M1 and M2 contained one and two DMA^+ units per noncharged repeat unit, respectively. Three copolymers containing NP side-arms (M1-PNP20, M1-PNP90, and M2-PNP60) were used (see Table 1). The numbers after PNP are the calculated side arm number-average molecular weights in kg/mol. M1-PNP90 has not been reported previously and was prepared using the same conditions as those described earlier.[21] Both families of cationic copolymer surfactants (M1-PMA and those based on PNP) had a pronounced tendency to adhere to anionic substrates and could not be analyzed using GPC. Following our previous work,[21−23] ^{1}H NMR spectroscopy was used to calculate the number-average molecular weight for the star-like copolymers studied. The preparation conditions and characterization data for M1-PNP20, M2-PNP60, and M1-PMA have been published earlier.[21,22] M1-PNP90 copolymer is new and characterization data appear in the Supporting Information (Figure S1). The mole ratio of NP to M1 used to prepare M1-PNP90 was 500. The molecular weight and composition data are shown in Table 1. M1-PMA contained repeat units of 2-(2-methoxyethoxy)-ethylmethacrylate (Table 1). The preparation and characterization of M1-PMA was described earlier.[22] Linear PNP and PVA were also used as polymer surfactants and were purchased (see above).

Table 1. Characterization Data for the Polymer Surfactants

abbreviation	composition[a]	M_n/(kg/mol)[b]	ref.
M1-PNP20	$PDMA^+_{23}$-*g*-$(PNP_{195})_{23}$	515	21
M1-PNP90	$PDMA^+_{23}$-*g*-$(PNP_{780})_{23}$	2,030	This work
M2-PNP60	$PDMA^+_{30}$-*g*-$(PNP_{570})_{14}$	918	21
M1-PMA	$PDMA^+_{23}$-*g*-$(PMA_{101})_{23}$	450	22
PNP	PNP_{220}[c]	25[c]	This work
PVA	PVA_{470}[d]	21[d]	This work

[a]Compositions were determined from ^{1}H NMR spectra for M-PNP and M1-PMA. [b]Determined from ^{1}H NMR spectra. [c]Calculated from supplier information for M_w. [d]Calculated from supplier information for M_n.

Colloidosome Preparation. There are three differences in the method used in the present study compared to other preparations of hollow particles involving solvent evaporation.[4,16] The first is that much higher oil phase volume fractions (ϕ_o) values were used here (typically 0.50 to 0.67, Table 2). Values for ϕ_o greater than or equal to 0.50 were essential for producing large emulsion droplets that transformed to colloidosomes upon CH_2Cl_2 evaporation. The highest proportions of colloidosomes were produced using ϕ_o of about 0.60 to 0.67. Second, dispersions with well-dispersed colloidosomes were only produced when the structural polymer solution was fed slowly into the aqueous phase. They could not be formed effectively using a conventional batch method. Rapid removal of CH_2Cl_2 was also required to accelerate phase separation and generate the particles that comprised the colloidosome shells. In each case a CH_2Cl_2/structural polymer solution (i.e., the polymer that would comprise the shell of the colloidosomes) was fed into an aqueous solution containing the polymer surfactant. Most of the colloidosome preparations were conducted using a small-scale preparation method. Larger-scale colloidosome preparations were also conducted.

dx.doi.org/10.1021/la402788a | *Langmuir* 2013, 29, 13676−13685

Table 2. Colloidosome Preparation Conditions Employed and Size Data

entry	scale	systems	V_w[a]/ mL	C_{Surf}[b]/ wt.%	V_o[c]/ mL	C_{Pol}[d]/ w/v%	ϕ_o[e]	D_n[f]/ μm
1	Small	PCL10/M1-PNP90	1.5	0.2	3.0	0.5	0.67	8.0
2	Small	PCL10/M1-PNP90	1.5	0.2	3.0	1.0	0.67	12
3	Small	PCL10/M1-PNP90	1.5	0.2	3.0	2.0	0.67	20
4	Small	PCL10/M1-PNP90	1.5	0.1	3.0	1.0	0.67	58
5	Small	PCL10/M1-PNP90	1.5	1.0	2.0	0.2	0.57	2.8
6	Small	PCL10/M1-PNP90	1.5	0.2	1.5	2.0	0.50	8.1
7	Small	PCL10/M1-PNP90	1.5	0.2	3.0	1.0	0.67	16
8	Small	PCL10/M1-PNP90	1.5	0.2	3.0	1.0	0.67	14
9	Small	PCL10/M1-PNP20	1.5	0.2	3.0	1.0	0.67	9.4
10	Small	PCL10/M2-PNP60	1.5	0.2	3.0	1.0	0.67	7.6
11	Small	PCL10/PNP	1.5	0.2	3.0	1.0	0.67	9.2
12	Small	PCL10/PVA	2.0	1.2	3.0	1.5	0.60	3.8
13	Small	PCL−OH/M1-PNP90	1.5	0.2	3.0	1.0	0.67	10
14	Small	PCL80/M1-PNP90	1.5	0.2	3.0	1.0	0.67	6.5
15	Small	PS35/M1-PNP90	1.5	0.2	3.0	1.0	0.67	13
16	Large	PCL10/M1-PMA	30	0.5	60	1.5	0.67	13
17	Large	PCL10/PVA	75	1.2	100	1.5	0.57	27

[a]Volume of water. [b]Polymer surfactant concentration. [c]Volume of oil phase. [d]Concentration of structural polymer. [e]Volume fraction of oil phase. [f]Number-average diameter.

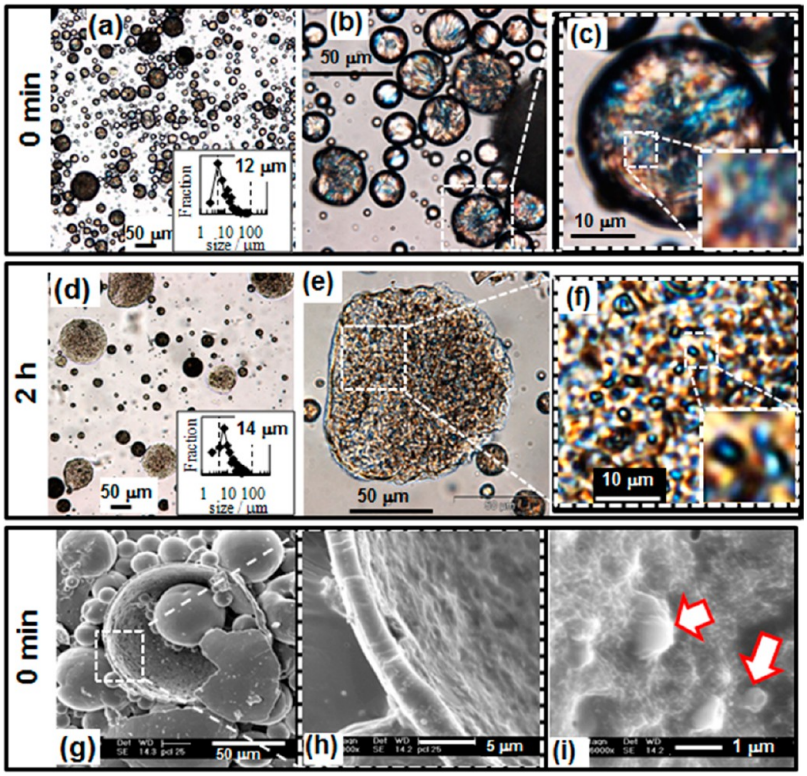

Figure 1. Effect of time delay prior to rotary evaporation for PCL10/M1-PNP90 colloidosomes. The time delays between the end of the feed and rotary evaporation are shown. The colloidosomes were prepared using the small-scale method (entry 2 of Table 2). For (a−c) and (g−i) the emulsion was rotary evaporated immediately after the end of the feed. The insets for (a) and (d) show the size distributions and values for D_n. SEM images for the colloidosomes from (a) are shown in (g−i). The arrows in (i) show particles that formed the colloidosome shell.

Small-Scale Colloidosome Preparation. A Silverson LR4 high shear mixer was used with a microtubular work-head (10 mm diameter). The following describes the preparation for PCL10 colloidosomes prepared in the presence of M1-PNP90 (Entry 2, Table 2). The colloidosome is termed PCL10/M1-PNP90. A solution of CH_2Cl_2 (3.0 mL) and PCL (1.0 w/v %) was added at a uniform rate using a syringe pump to 1.5 mL of water containing M1-PNP90 (0.2 wt.%) over a period of 30 min using high shear (9000 rpm). The mixture was cooled in an ice water bath during emulsification. After the feed, the emulsion was immediately rotary evaporated at room temperature to remove CH_2Cl_2 and trigger colloidosome formation. Further details of the conditions used to prepare the other colloidosomes studied appearing in Table 2. When required, pyrene was added to the CH_2Cl_2 before emulsification at a concentration of ca. 0.075 wt.% with respect to structural polymer.

Larger-Scale Colloidosome Preparation. A Silverson LR4 high shear mixer was used with a batch work-head (50 mm diameter) fitted with an emulsifior screen. An example method for a larger-scale

dx.doi.org/10.1021/la402788a | Langmuir 2013, 29, 13676−13685

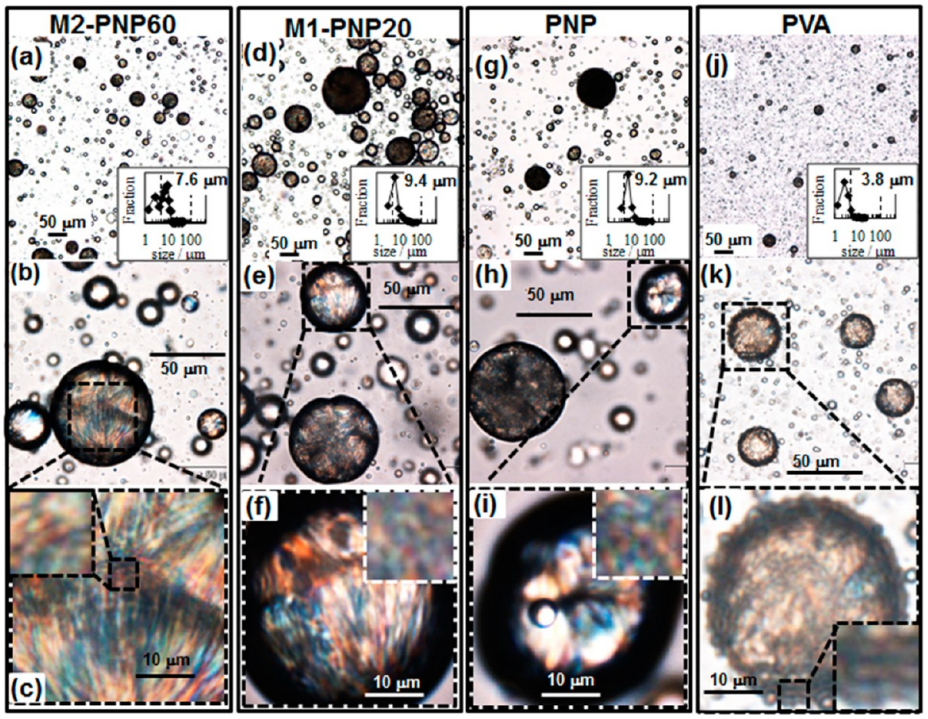

Figure 2. Optical microscopy images showing effects of polymer surfactant type for PCL10 colloidosomes. The identities of the polymer surfactants are shown. M2-PNP60, M1-PNP20, PNP, and PVA correspond to entries 10, 9, 11, and 12 in Table 2. The insets in the bottom row have sizes of 5 × 5 μm^2.

preparation is provided for PCL10 colloidosomes prepared in the presence of M1-PMA, i.e., PCL10/M1-PMA (Entry 16, Table 2). A solution of CH_2Cl_2 (60 mL) and PCL (1.5 w/v %) was added at a uniform rate using a syringe pump to 30 mL of water containing M1-PMA (0.5 wt.%) over a period of 30 min with high shear (10,000 rpm). The mixture was cooled in an ice−water bath during emulsification. After the feed the emulsion was mixed using a magnetic stirrer for 1 h. It was then rotary evaporated at room temperature to remove CH_2Cl_2 and trigger colloidosome formation.

Physical Measurements. The yields of dispersed particles (colloidosomes and nonadsorbed particles) were determined gravimetrically using freeze-dried dispersions. An Olympus BX41 microscope was used to obtain optical images. For a given sample, a drop of as-prepared dispersion was placed on a microscope slide and was viewed immediately. All optical microscopy images were obtained using transmitted light. The light passed through a polarizer and an analyzer. For all measurements in this work the analyzer was fixed at an angle of approximately 30° with respect to the polarizer unless otherwise stated. The objective lenses used had magnifications of ×5, ×40, and ×60. Number-average sizes (D_n) were determined by counting at least 100 colloidosomes. SEM measurements were obtained using a Philips FEGSEM instrument. Samples were dried at room temperature or by freeze-drying. When required, samples were crushed at liquid nitrogen temperature (see text). Colloidosomes containing pyrene were studied using a Nikon Eclipse 50i fluorescence microscope equipped with a 60-fold magnification oil-immersion objective. Experiments involving pyrene used a DAPI filter which allowed transmission of light at 475 nm.

RESULTS AND DISCUSSION

Effects of Time Delay Prior to Rotary Evaporation. We discovered that colloidosomes could be prepared using solvent evaporation if high ϕ_o values were employed (0.60 to 0.67) and rotary evaporation was used to accelerate CH_2Cl_2 removal. A slow, uniform feed of the structural polymer solution was essential. Figure 1a−c shows optical images of PCL10/M1-PNP90 colloidosomes where rotary evaporation was conducted immediately after the CH_2Cl_2/PCL solution feed. The size distribution was polydisperse. (More narrow size distributions were achieved using the larger scale mixing head (Figures 6 and 7.) There were two types of particles present: large hollow colloidosomes and smaller particles.

Interestingly, the larger colloidosomes that formed after rotary evaporation were colored when viewed by optical microscopy (see Figure 1c and f). Polarized light was used for all optical microscopy data presented in this study. The inset of Figure 1c (and Figure S2) reveals that the colloidosome shell comprised smaller particles with a size of about 1 μm. The origin of the colors for these shell-particles will be discussed later. An image of the colloidosomes (Figure S2) showed that smaller colloidosomes could be seen behind the larger colloidosomes. This demonstrates that the colloidosomes were hollow. In the following we show results from studies of key variables that influenced the proportion of colloidosomes obtained. We mostly assessed the proportion of colloidosomes present by optical microscopy. This was supported by gravimetric measurements to determine yield.

If the time between the end of the feed and rotary evaporation increased, then the size and the proportion of PCL10/M1-PNP90 colloidosomes also increased. However, their yield decreased. Figure 1d and e shows images of colloidosomes formed after 2 h of stirring. Larger colloidosomes were produced (though aggregation) that occurred during the delay between the end of the feed and accelerated removal of CH_2Cl_2 by rotary evaporation. For this system the particles that made up the shells of the colloidosomes were distinct (see inset of Figure 1f). For PCL10/M1-PNP90, rotary evaporation immediately after emulsification gave the highest proportion of colloidosomes with shells formed from partially coalesced particles (Figure 1a−c). The yield of particles was

dx.doi.org/10.1021/la402788a | Langmuir 2013, 29, 13676−13685

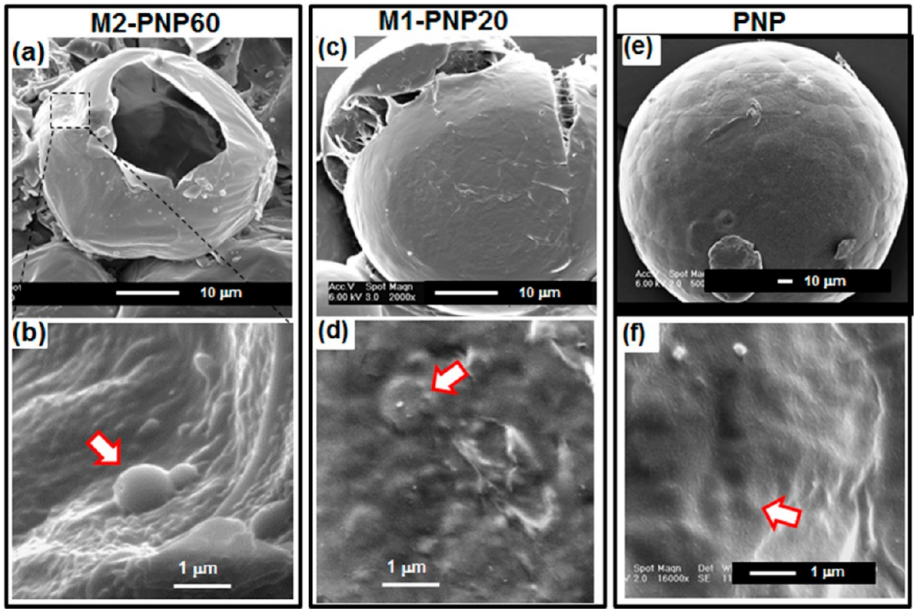

Figure 3. SEM images showing effects of polymer surfactant type for PCL10 colloidosomes. The identity of the polymer surfactants are shown. M2-PNP60, M1-PNP20, and PNP correspond to entries 10, 9, and 11 in Table 2. The lower images are higher magnifications of sections of the colloidosome surfaces. The arrows highlight particles that comprised the shell. Smaller, submicrometer-sized particles were also evident.

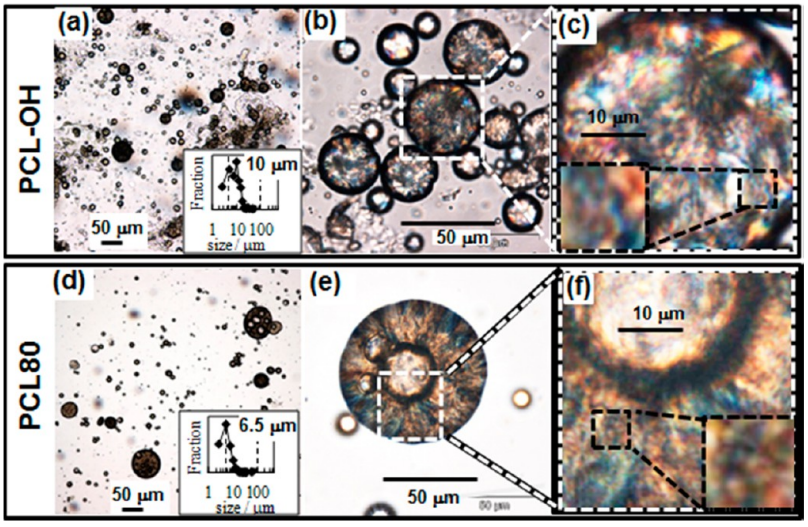

Figure 4. Effects of structural polymer type. The structural polymer used is indicated. The polymer surfactant was M1-PNP90. The PCL-OH/M1-PNP90 and PCL80/M1-PNP90 systems correspond to entries 13 and 14, respectively, of Table 2.

about 68 wt.%. Rotary evaporation was also accompanied by an increase in dispersion stability.

SEM images for the PCL10/M1-PNP90 colloidosomes were obtained (Figure 1g–i). The shell thickness (from Figure 1h) was about 1.5 μm and a shell-to-diameter ratio was estimated at ~0.01. The high magnification image of the inside wall (Figure 1i) shows that the colloidosome shell was composed of partially fused particles. This is further evidence that our method produced colloidosomes.

Effects of Polymer Surfactant Concentration and Type. The polymer surfactant concentration (C_{surf}) played an important role in colloidosome preparation. The value for C_{surf} used for Figure 1 was 0.2 wt.%. However, when a lower C_{surf} value of 0.1 wt.% was used, much larger PCL10/M1-PNP90 colloidosomes were produced in low yield (see Figure S3(a) and (b)). If a high C_{surf} value was used (e.g., 1.0 wt.%) then mostly small conventional (nonhollow) particles were produced (see Figure S3(c) and (d)). It was only when C_{surf} was not sufficient to permit formation of a fine O/W emulsion using our conditions that colloidosomes were produced.

Our method enabled colloidosomes to be prepared using other polymer surfactants (Figure 2). It can be seen from Figures 1 and 2 that the D_n values were comparable for all polymer surfactants containing NP segments (7.6–12 μm). Although colloidosomes could be prepared using commercially available PNP, the yield of colloidosomes was relatively low (as judged by optical microscopy) due to significant coagulum formation. Gravimetric data showed a particle yield of about 20 wt.% for the PCL10/PNP system. The ability of PNP to act as a surfactant must originate from the combination of hydrophilic (amide) and hydrophobic (isopropyl) groups within each repeat unit. PNP is significantly surface active.[24] PVA (also

dx.doi.org/10.1021/la402788a | *Langmuir* 2013, 29, 13676–13685

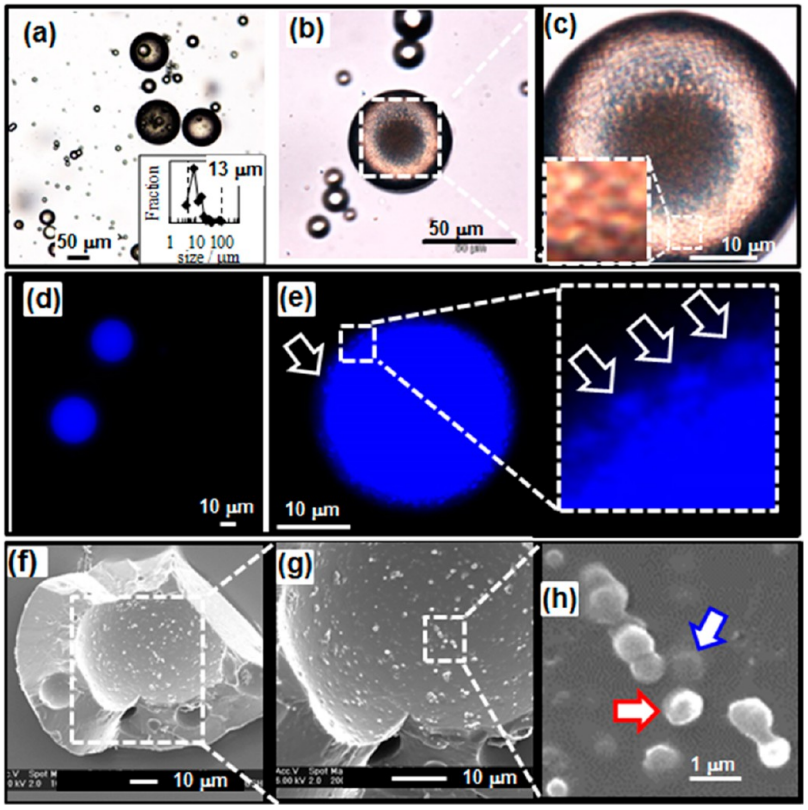

Figure 5. PS35/M1-PNP90 colloidosomes. The polymer surfactant was M1-PNP90. The system corresponds to entry 15 of Table 2. (d) and (e) show fluorescence images of pyrene loaded colloidosomes. The arrows in (e) highlight shell-particles. (f) to (h) show SEM images of crushed colloidosomes. For (h) the red and blue arrows indicate particles present at the shell surface and within the shell, respectively.

commercially available) is more highly surface active and gave a much smaller particle size. An increase of the structural polymer concentration (C_{Pol}) to 1.5 w/v% (entry 12, Table 2) was used to prepare colloidosomes (Figure 2j–l).

The higher magnification optical microscopy images for PCL10/M2-PNP60 and PCL10/M1-PNP20 showed aligned colored stripes (Figure 2c and f). The insets for Figure 2c,f,i,l show that the colloidosome shells were comprised of particles. We propose that the colored stripes resulted from stress-induced buckling that occurred within the shells during solvent evaporation. This would have altered the packing of the particles comprising the shell.

SEM images for PCL10/M2-PNP60 colloidosomes were obtained using samples that had been crushed by a spatula under liquid nitrogen (Figure 3a and b). Figure 3a shows a shell and confirms that the PCL colloidosomes were hollow. The higher magnification image (Figure 3b) shows that the shell wall comprised small particles. SEM images for PCL10/M1-PNP20 and PCL10/PNP colloidosomes are also shown in Figure 3. The lower magnification image for PCL10/PNP (Figure 3e) shows evidence of large shell-particles and aggregates that had partially fused. The higher magnification images for PCL10/M1-PNP20 and PCL10/PNP (Figure 3d and f) also show that the shells were composed of partially fused small particles (red arrows). The shell-particles are less distinct when examined by SEM because the colloidosomes were dehydrated and the contrast between the particles and the polymer surfactant that is proposed to have separated them was diminished.

Effect of Structural Polymer Concentration and Type. The size and proportion of the colloidosomes increased with C_{Pol} (see Figure S4). Increased C_{Pol} values caused precipitation within the oil droplets at an earlier stage of CH_2Cl_2 evaporation and this increased D_n. For the small-scale PCL10/M1-PNP90 colloidosome preparations, conditions that gave stable dispersions with a majority of colloidosomes with a size in the range of about 5–100 μm were those for entry 2 in Table 2 (D_n = 12 μm). This size range is desirable for colloidosomes from the viewpoints of verifying their presence using optical microscopy and also fluorescence microscopy (below). This size range includes the sizes often reported for colloidosomes.[1]

The effect of structural polymer type was also investigated (see Figures 4 and 5). Compared to PCL10/M1-PNP90 (Figure 1a–c), aggregation was more pronounced for PCL-OH/M1-PNP90 (Figure 4a) and PCL80/M1-PNP90 (Figure 4d). This gave a decreased proportion of colloidosomes as judged by the respective size distributions. An optimum molecular weight range of 10 kg/mol for PCL applied in terms of maximizing colloidosome yield. Because solvent evaporation occurs within the droplet periphery, it is the periphery of the droplets which would have had the highest local PCL concentration as a result of solvent evaporation in the absence of rapid diffusion. The viscosity of the CH_2Cl_2 phase would have increased with structural polymer molecular weight. We propose that a highly viscous (sticky) shell favored excessive aggregation of larger droplets during solvent evaporation, which decreased colloidosome yield. Occasional buckled colloidosomes were evident for PCL80/M1-PNP90 (see Figure 4e), which is due to stress imbalances within the shell during contraction due to CH_2Cl_2 evaporation.

Colloidosomes were also prepared using PS35 as the structural polymer (Figure 5a–c). The particle yield was 60

dx.doi.org/10.1021/la402788a | *Langmuir* 2013, 29, 13676–13685

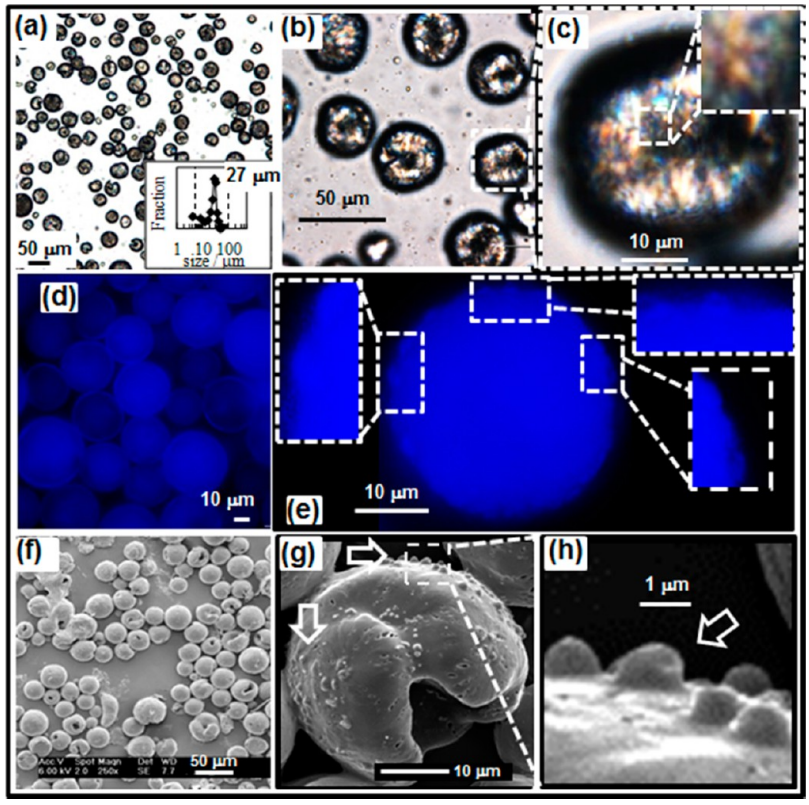

Figure 6. PCL10/PVA colloidsome preparations conducted at larger scale. Optical microscopy images and size distributions are shown in (a–c). Fluorescence images of pyrene loaded colloidosomes are shown in (d) and (e). SEM images of the colloidosomes are shown in (f–h). The colloidosome corresponds to entry 17 in Table 2. The arrows in (e) and (h) indicate shell-particles.

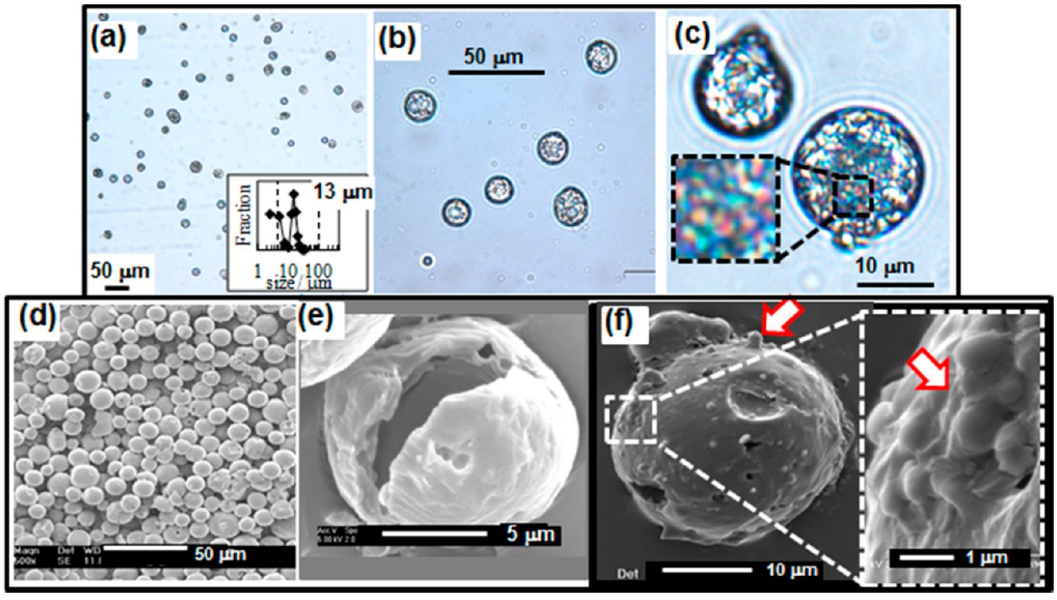

Figure 7. PCL10/PMA colloidsome preparations conducted at larger scale. Optical microscopy images and a size distribution are shown in (a–c). SEM images of the colloidosomes are shown in (d–f). The colloidosome corresponds to entry 16 in Table 2. The arrows in (f) indicate shell-particles.

wt.% as determined by gravimetric measurement. The PS35/M1-PNP90 colloidosomes showed very good examples of a shell (Figure 5b and c). The highest magnification optical microscopy images showed shell-particle separations of the order of visible light (Figure 5c, inset). The presence of shell-particles of about 1 μm in size in the shell was confirmed for pyrene-loaded PS35/M1-PNP90 colloidosomes using fluorescence microscopy (see Figure 5d and e). The arrow in the inset of Figure 5e identifies the outermost shell-particles and confirms that colloidosomes were prepared.

SEM images were obtained for crushed PS35/M1-PNP90 particles (see Figure 5f–h). The shell thickness was 18 μm and

dx.doi.org/10.1021/la402788a | *Langmuir* 2013, 29, 13676–13685

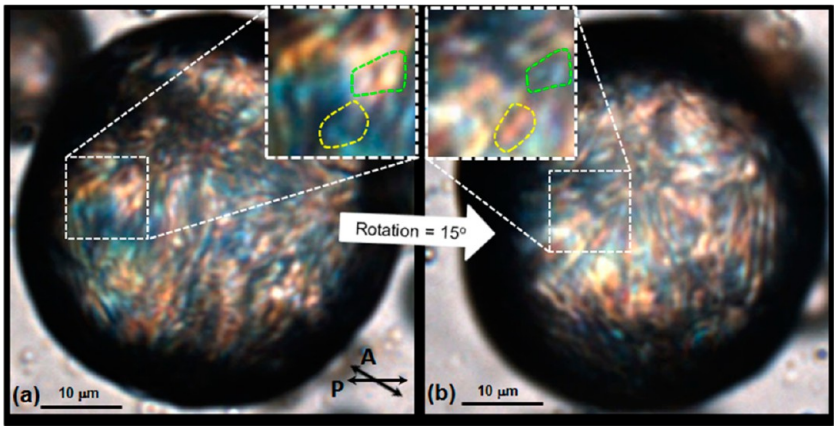

Figure 8. Color changes with PCL colloidosome rotation. Optical microscopy images showing a PCL10/M2-PNP60 colloidsome that had rotated left-to-right by about 15° along its equator. Different parts of the surface changed color as a result of colloidosome rotation. Examples of small shell-particles that changed color are highlighted in the insets. The overlapping double headed arrows in (a) show the polarizer (P) and analyzer (A) orientations used in this work.

the shell thickness to diameter ratio was about 0.30. An increased shell thickness implies a higher structural polymer concentration within the larger droplets that formed colloidosomes. This may originate from more pronounced adsorption of small droplets onto the larger colloidosome-forming droplets during colloidosome formation (Scheme 1). The smaller droplets at the periphery evaporated first due to their size and delivered polymer into the surface of larger droplets which evaporated more slowly. The higher magnification images (Figure 5g and h) show small particles were present. Many of these particles were partially fused and present within the shells (blue arrow in Figure 5h). We propose that the shells comprised PCL particles dispersed within a polymer surfactant matrix. Drying of the samples for SEM caused contraction of the polymer surfactant phase (due to water evaporation) and a loss of contrast between the two phases. This is why the particles that comprise the colloidosome shells were less distinct when examined by SEM compared to optical and fluorescence microscopy.

Effects of Preparation Scale. We scaled up the preparation of PVA-stabilized colloidosomes using the larger scale mixing geometry (see Experimental section). Figure 6 shows optical microscopy, fluorescence microscopy and SEM images from entry 17 (Table 2). Compared to the small-scale preparation (entry 12, Table 2, 3.8 μm), the larger-scale preparation (Figure 6a) gave larger colloidosomes (27 μm) with a more narrow size distribution. The larger scale mixing geometry produced a uniform shear across the whole emulsion. The yield of colloidosomes increased from 29 wt.% (small scale) to 83 wt.% (larger scale) as judged by gravimetric measurement. The inset of Figure 6c shows that the shells comprised smaller particles. We also prepared colloidosomes containing pyrene (see Figure 6d and e) and a shell was present. The higher magnification images showed that small particles were present at the periphery (inset of Figure 6e). SEM images revealed small particles (arrows in Figure 6g and h) on the PCL10/PVA colloidosome surface. Other images showed nanoparticles embedded within the surface (Figure S5(a) − (c)). This supports our view that the shells of the hollow colloidosomes contained partially fused PCL particles. We note that birefringent shell particles were also apparent using cross-polarized light. In that case the angle between the polarizer and analyzer was 90° (this can be seen from PCL10/PVA colloidosome images in Figure S5(d) and (e)).

As a final test for generality of our approach we prepared PCL10/M1-PMA colloidosomes using the large-scale mixer. M1-PMA was shown earlier to be a thermally responsive polymer[22] and did not contain NP. Images of the colloidosomes are shown in Figure 7. The colloidosomes had low polydispersity. The inset of Figure 7c shows the presence of small particles within the shell. SEM images are shown in Figure 7d−f. Figure 7e shows that the colloidosomes were hollow. The inset of Figure 7f shows small particles that comprise the colloidosome shell. The particles evident in the inset of Figure 7f are of comparable size to those evident in the inset of Figure 7c. This methacrylate-based system is a promising candidate for future biomaterial study and potential application because the thermally responsive polymer has shown good thermal reversibility and is amide-free.[22]

Proposed Origin of the Colloidosome Shell Colors. We noticed that the colors of the particles that comprised the colloidosome shells changed with orientation of the colloidosome with respect to the transmitted polarized light direction. This is illustrated in Figure 8 for images of a PCL10/M2-PNP60 colloidosome that had rotated left-to-right by about 15° along its equator. Many of the surface regions changed color as a consequence of colloidosome rotation. The insets show magnified regions of the same shell regions before (Figure 8a) and after (Figure 8b) the rotation. Individual shell-particles that changed color from blue to red (highlighted by yellow dashed outlines) or orange to blue (highlighted by green dashed outlines) are evident. An angular dependent color observed using polarized light is a strong indication of birefringence.[25] Birefringence is well-known for PCL,[26,27] which is a semi-crystalline polymer.[26]

The particle colors evident within the PCL colloidosome shells probably originates from shear-induced stresses during fast solvent evaporation. Related studies have shown that fast evaporation of solvent during electrospinning of polysiobutylene-based elastomers can give birefringence.[25] In the present study, the local strain is proposed to have been "frozen in" during accelerated solvent evaporation and formation of the particles at the shell. Accordingly, the distinct colors of the particles in the colloidosome shells (e.g., inset of Figure 7c)

dx.doi.org/10.1021/la402788a | *Langmuir* 2013, 29, 13676−13685

imply a preferred orientation of the semicrystalline regions of the PCL within the shell-particles.

CONCLUSIONS AND OUTLOOK

We have demonstrated a new, simple method for colloidosome preparation. The generality of our approach, and hence high potential impact, was demonstrated by using commercially available materials (PS, PVA, and PNP). The use of accelerated evaporation of the solvent was crucial to locking in partially fused particles within the colloidosome shells. It was a combination of controlled aggregation/coalescence and kinetic trapping of precipitated nanoparticles that yielded colloidosomes. The colloidosome shells were proposed to consist of small particles (less than or equal to about 1 μm) which were separated by polymer surfactant. They appeared to be partially fused when viewed by SEM. Optical microscopy using polarized light showed that the PCL colloidosomes were birefringent, which was proposed to be due to frozen-in shear-induced stresses that occurred during shell-particle formation that gave preferred orientations of semicrystalline chains within the particles. The study showed the benefits of increasing the scale, which were a narrowed size distribution and improved colloidosome yield. Much larger scale preparations of colloidosome than used here are feasible in principle. The PCL10/PVA colloidosomes studied here is a potentially important system for biomaterial use because PCL and PVA are generally regarded as safe materials for use in the body. Hollow biodegradable particles have been shown to be beneficial for cartilage repair.[28] The presence of crystalline PCL regions may provide additional benefits for biomaterial application. First, these features may provide micrometer-scale, directional interactions with cells and tissue that are not normally present in conventional dispersions used for cell delivery. Second, they may result in enhanced elasticity of the colloidosomes. The use of thermally responsive polymer surfactants implies that new thermally responsive colloidosome dispersions could be prepared and this will be examined in future work.

ASSOCIATED CONTENT

Supporting Information

This provides M1-PNP90 copolymer composition from ^{1}H NMR spectroscopy and optical micrographs for various colloidosomes. This material is available free of charge via the Internet at http://pubs.acs.org.

AUTHOR INFORMATION

Corresponding Author

*E-mail: brian.saunders@manchester.ac.uk.

Notes

The authors declare no competing financial interest.

ACKNOWLEDGMENTS

We would like to thank the Malaysian Ministry of Higher Education and Universiti Malaysia Kelantan for funding. This work was in part funded by the EPSRC Centre for Innovative Manufacturing in Regenerative Medicine. Research leading to these results received funding from the European Research Council under the European Community's Seventh Framework Programme (FP7/2007-2013)/ERC grant agreement 227845 and also the EPSRC (grants EP/H005625/1 and EP/H028277/1). We would like to thank the referees for their helpful comments regarding this manuscript.

REFERENCES

(1) Yow, H. N.; Routh, A. F. Formation of liquid core-polymer shell microcapsules. *Soft Matter* **2006**, *2*, 940.
(2) Velev, O. D.; Furusawa, K.; Nagayama, K. Assembly of latex particles by using emulsion droplets as templates. 1. Microstructured hollow spheres. *Langmuir* **1996**, *12*, 2374.
(3) Jiang, S.; Granick, S. Controlling the geometry (Janus balance) of amphiphlic colloidal particles. *Langmuir* **2008**, *24*, 2438.
(4) Loxley, A.; Vincent, B. Preparation of poly(methylmethacrylate) microcapsules with liquid cores. *J. Colloid Interface Sci.* **1998**, *208*, 49.
(5) Dowding, P. J.; Atkin, R.; Vincent, B.; Bouillot, P. Oil core-polymer shell microcapsules prepared by internal phase separation from emulsion droplets. I. Characterization and release reates for microcapsules with polystyrene shells. *Langmuir* **2004**, *20*, 11374.
(6) Cayre, O.; Noble, P. F.; Paunov, V. N. Fabrication of novel colloidosome microcapsules with gelled aqueous cores. *J. Mater. Chem.* **2004**, *14*, 3351.
(7) McClements, D. J. Advances in fabrication of emulsions with enhanced functionality using structural design principles. *Curr. Opin. Colloid Interface Sci.* **2012**, *17*, 235.
(8) Keen, P. H. R.; Slater, N. K. H.; Routh, A. F. Encapsulation of lactic acid bacteria in colloidosomes. *Langmuir* **2012**, *28*, 16007.
(9) Thompson, K. L.; Glakoumatos, E. C.; Ata, S.; Webber, G. B.; Armes, S. P.; Wanless, E. J. Direct observation of giant pickering emulsion and colloidosome droplet interaction and stability. *Langmuir* **2012**, *28*, 16501.
(10) Dinsmore, A. D.; Hsu, M. F.; Nikolaides, M. G.; Marquez, M.; Bausch, A. R.; Weitz, D. A. Colloidosomes: selectively permeable capsules composed of colloidal particles. *Science* **2002**, *298*, 1006.
(11) Bon, S. A. F.; Cauvin, S.; Colver, P. J. Colloidosomes as micron-sized polymerisation vessels to create supracolloidal interpenetrating polymer network reinforced capsules. *Soft Matter* **2007**, *3*, 194.
(12) Li, W.; Zhao, C.; Tan, J.; Jiang, J.; Xu, J.; Sun, D. Roles of methyl orange in preparation of emulsions stabilized by layered double hydroxide particles. *Colloids Surf., A* **2013**, *421*, 173.
(13) Minami, H.; Kanamori, H.; Hata, Y.; Okubo, M. Preparation of microcapsules containing a curing agent for epoxy resin by polyaddition reaction with the self-assembly of phase-separated polymer method in an aqueous dispersed system. *Langmuir* **2008**, *24*, 9254.
(14) Horecha, M.; Senkovskyy, V.; Stamm, M.; Kiriy, A. One-pot synthesis of thermoresponsive PNIPAM hydrogel microcapsules designed to function in apolar media. *Macromolecules* **2009**, *42*, 5811.
(15) Caruso, F.; Caruso, R. A.; Mohwald, H. Nanoengineering of Inorganic and Hybrid Hollow Spheres by Colloidal Templating. *Science* **1998**, *282*, 1111.
(16) Kim, Y. B.; Yoon, K.-S. A physical method of fabricating hollow polymer spheres directly from oil/water emulsions of solutions of polymers. *Macromol. Rapid Commun.* **2004**, *25*, 1643.
(17) Park, C. H.; Lee, J. Electrosprayed polymer particles: effect of the solvent properties. *J. Appl. Polym. Sci.* **2009**, *114*, 430.
(18) Bird, R.; Freemont, T. J.; Saunders, B. R. Hollow polymer particles that are pH-responsive and redox sensitive: two simple steps to triggered particle swelling, gelation and disassembly. *Chem. Commun.* **2011**, *47*, 1443.
(19) Maglio, G.; Nicodemi, F.; Conte, C.; Palumbo, R.; Tirino, P.; Panza, E.; Lanaro, A.; Ungaro, F.; Quaglia, F. Nanocapsules based on linear and Y-shaped 3-Miktoarm star-block PEO-PCL copolymers as sustained delivery system for hydrophilic molecules. *Biomacromolecules* **2011**, *12*, 4221.
(20) Katz, J. S.; Elsenbrown, K. A.; Johnston, E. D.; Kamat, N. P.; Rawson, J.; Therien, M. J.; Burdick, J. A.; Hammer, D. A. Soft biodegradable polymerosomes from caprolactone-derived polymers. *Soft Matter* **2012**, *8*, 10853.
(21) Liu, R.; De Leonardis, P.; Cellesi, F.; Tirelli, N.; Saunders, B. R. Cationic temperature-responsive poly(N-isopropyl acrylamide) graft

copolymers: from triggered association to gelation. *Langmuir* **2008**, *24*, 7099.
(22) Shahidan, N.; Liu, R.; Cellesi, F.; Alexander, C.; Shakesheff, K. M.; Saunders, B. R. Thermally triggered assembly of cationic graft copolymers containing 2-(2-methoxyethoxy)ethyl methacrylate side chains. *Langmuir* **2011**, *27*, 13868.
(23) Shahidan, N.; Alexander, C.; Shakesheff, K. M.; Saunders, B. R. Gelation of microsphere dispersions using a thermally-responsive graft polymer. *J. Colloid Interface Sci.* **2013**, *396*, 187.
(24) Richardson, R.; Pelton, R.; Cosgrove, T.; Zhang, J. A neutron reflectivity study of poly(N-isopropylacrylamide) at the air-water interface with and without sodium dodecyl sulfate. *Macromolecules* **2000**, *33*, 6269.
(25) Lim, G. T.; Puskas, J. E.; Reneker, D. H.; Jakli, A.; Horton, W. E. Highly hydrophobic electrospun fiber mats from polyisobutylene-based thermoplastic elastomers. *Biomacromolecules* **2011**, *12*, 1795.
(26) Krishnanand, K.; Deopura, B. L.; Gupta, B. Determination of intrinsic birefringence values of polycaprolactone filaments. *Polym. Int.* **2013**, *62*, 49.
(27) Floudas, G.; Hilliou, L.; Lellinger, D.; Alig, I. Shear-induced crystallization of poly(e-caprolactone). 2. evolution of birefringence and dichroism. *Maromolecules* **2000**, *33*, 6466.
(28) Liu, X.; Jin, X.; Ma, P. X. Nanofibrous hollow microspheres self-assembled from star-shaped polymers as injectable cell carriers for knee repair. *Nat. Mater.* **2011**, *10*, 398.